AIAA JOURNAL
Vol. 35, No. 8, August 1997

Dynamic Buckling of Imperfect Cylindrical Shells Under Axial Compression and Bending Moment

Xiaozhi Huyan* and George J. Simitses†
University of Cincinnati, Cincinnati, Ohio 45221

The dynamic stability of circular metallic and laminated cylindrical shells is investigated. The cylinders are geometrically imperfect and subjected to axial compression or pure bending moment. These loads are suddenly applied with constant magnitude and finite or infinite duration. The finite element method is employed to generate dynamic responses and the equations of motion approach to determine dynamic critical loads. The effects of load duration and imperfection amplitude on critical loads are discussed. It is found that the dynamic critical loads decrease with increasing load duration and converge to those for the load case of infinite duration. The convergence rate is related to the fundamental frequency of the cylinder. In addition, both the static and dynamic critical loads decrease with increasing imperfection amplitude.

I. Introduction

THE problem of dynamic stability of circular cylindrical shells has been studied by many researchers, and it encompasses many classes of problems and many physical phenomena. Parametric resonance or parametric excitation,[1–3] pulse buckling,[4–6] and solid–fluid interaction[7] represent but a few subjects of these studies. See, for example, the review papers by Svalbonas and Kalnins,[8] Hsu,[9] and Simitses.[10]

The dynamic buckling of cylindrical shells subjected to suddenly applied axial compression of constant magnitude and infinite duration was first studied in Ref. 11, where a two-degree-of-freedom system was modeled and the Galerkin method was employed. Roth and Klosner[12] applied the potential energy method and treated the problem as a four-degree-of-freedom system that they studied numerically. Using the same model and the Budiansky–Roth[13] criterion, Tamura and Babcock[14] presented dynamic critical loads of an imperfect thin circular cylindrical shell. Their analysis included the effect of axial inertia and of an attached mass on the loaded edge of the shell. Moreover, they provided results for $L/R = 2$ and $R/h = 1000$ and various values of the initial imperfection, which were experimentally established. Based on their work, Simitses[15] investigated the effect of static preloading on the dynamic critical load. He employed the total potential energy approach to estimate critical conditions. The dynamic buckling analysis of laminated cylindrical shells under the same loading condition was also performed by him.[16]

The dynamic buckling of imperfect circular metallic and laminated cylinders is studied in this paper and the following points are emphasized.

1) The cylinders are subjected to two dynamic loads: axial compression or pure bending moment (Fig. 1).

2) Two load models are established for each load case: axial compression and pure bending moment. One is the suddenly applied load with finite duration (load model 1) and the other is suddenly applied load with infinite duration (load model 2). In all cases, the load is constant in magnitude (see Fig. 2 and note that T denotes the value of load duration).

3) The effects of imperfection shape and amplitude, and load duration on dynamic critical loads are considered.

Received Sept. 12, 1996; revision received April 25, 1997; accepted for publication May 11, 1997.

*Research Assistant, Department of Aerospace Engineering and Engineering Mechanics; currently Senior Specialist, Standard Body Fuselage Programs, Boeing Aircraft Co., MS K65-52, P.O. Box 7730, Wichita, KS 67277. Member AIAA.

†Professor, Department of Aerospace Engineering and Engineering Mechanics. Fellow AIAA.

The dynamic buckling is assumed to occur in the load duration. There exist instances where dynamic buckling in a structure occurs after large time compared to the duration of the applied load.[17,18] Such a possibility is excluded in the present study.

II. Methodology

A. Criteria for Dynamic Critical Conditions

There are three methods used by the various investigators in estimating critical conditions for dynamically loaded elastic systems. They are the total energy-phase plane approach,[19–21] the total potential energy approach,[21,22] and the equations of motion approach.[13] Their concepts and details are described as follows.

1. *Total Energy-Phase Plane Approach*

Critical conditions are related to characteristics of the system phase plane, and the emphasis is on establishing sufficiency conditions for stability (lower bounds) and sufficiency conditions for instability (upper bounds). For a one-degree-of-freedom system, the energy balance equation is plotted in the phase plane for various values of the load parameter. When load parameters are small, the curve is a closed one and the motion is bounded and, therefore, it is stable. As the load parameter is increased, a value is reached at which an escaping motion is possible and the system is in critical condition.

2. *Total Potential Energy Approach*

Critical conditions are related to characteristics of the system total potential. Through this approach, also, the lower and upper bounds of critical conditions are established. The energy balance equation is used and the total potential is plotted vs the system generalized coordinates for various values of the load parameter in this approach. When escaping motion is possible, a critical condition exists.

3. *Equations of Motion Approach*

The equations of motion are numerically solved for various values of the load parameter, thus obtaining system responses. The load parameter, at which there exists a large change in responses, is called critical. This approach is easily adapted to computational methods such as finite element codes and, therefore, it has become very popular in application. In addition, it has met with success when applied to systems that exhibit violent buckling (limit point and bifurcation point with unstable postbuckling branch) under static loads. Cylindrical shells are typical violent buckling configurations.[16] Hence, this criterion is employed in the present work.

B. Finite Element Method

There are four approaches[23] to applying finite element methods for analyzing shell structures: 1) general three-dimensional elements could be used, 2) the shell structure is faceted with flat elements, 3) one of several shell theories is employed to develop a curved-shell

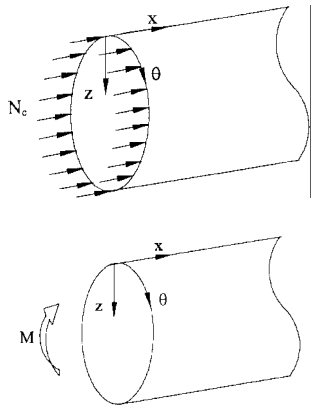

Fig. 1 Cylinders under axial compression or pure bending moment.

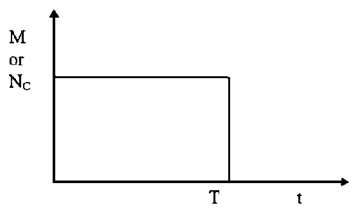

Finite duration, load model 1

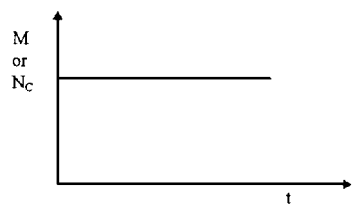

Infinite duration, load model 2

Fig. 2 Suddenly applied load with constant magnitude.

element, and 4) the curved-shell elements are formed by degenerating the three-dimensional strain-displacement relations. Inasmuch as a shell is characterized by the dimension in the thickness direction being smaller than the in-plane dimensions, numerical ill conditioning may result by using three-dimensional elements to model shell structures. Additionally, many degrees of freedom would be involved, which may not be necessary. Approach 2 must contend with discontinuous bending moments between elements and achieves convergence only for fine meshes. The acceptance of approach 3 has been hindered due to the absence of a general nonlinear shell theory. Approach 4 is perhaps the most popular method and first appeared in the form of the Ahmad et al.[24] element. They are superparametric elements and can exactly simulate parabolic curved shells. Moreover, the transverse displacements and rotations are treated independently in elements of this type and, hence, they are well suited to thick cylindrical shells and laminated cylindrical shells by the aid of shear deformation theories. Hence, the element of this type is employed to obtain the response of a cylindrical shell under a dynamic load. The ANSYS computer code is chosen, and the analysis procedures are the same as those used in Ref. 25. For completeness, the stress resultant acting on the ends of a cylinder is given by

$$N_{(\theta)} = N_c + N_b \cos(\theta) \tag{1}$$

where N_b is the maximum load per unit circumference due to bending moment

$$M = \pi R^2 N_b \tag{2}$$

and N_c is the axial compression load per unit of circumference. The cylinder is under pure bending if $N_c = 0$ and under pure compression if $N_b = 0$. The end load is transferred to equivalent nodal forces in the finite element model.[25] The dynamic critical compression load and bending load are represented by $(N_c)_d$ and $(N_b)_d$, respectively. Moreover, two eight-node elements are selected to include the effect of transverse shear deformation, and the reduced shear moduli are used in the formation of stiffness matrices to avoid shear locking for thin cylinders.

In the dynamic analysis, the basic equations of motion of a cylindrical shell are

$$[M]\{\ddot{u}\} + [C]\{\dot{u}\} + [K]\{u\} = \{F(t)\} \tag{3}$$

where $[M]$ = mass matrix, $[C]$ = damping matrix, $[K]$ = stiffness matrix, including nonlinearity, $\{\ddot{u}\}$ = nodal acceleration vector, $\{\dot{u}\}$ = nodal velocity vector, $\{u\}$ = nodal displacement vector, and $\{F(t)\}$ = load vector. After replacing the time derivatives $\{\dot{u}\}$ and $\{\ddot{u}\}$ with differences of displacement $\{u\}$ at various instants of time by using the Newmark time integration scheme,[26] these equations can be thought of as a set of static equilibrium equations that also take into account inertia forces $[M]\{\ddot{u}\}$ and damping forces $[C]\{\dot{u}\}$. They are solved with the aid of the Newton–Raphson procedure.[27] In the direct integration method, the time increment between successive time points is called the integration time step. Because the response can be thought of as a combination of modes, the time step should be able to resolve the highest mode that can contribute to the response. It has been found that using approximately 20 points per period of the highest frequency of interest results in a reasonably accurate solution. That is, if f_i is the frequency of the highest considered mode, the time integration step ΔT is given by

$$\Delta T \leq 1/20 f_i \tag{4}$$

In the present analysis, the effect of damping is ignored and all the initial displacements and velocities are set to be zero.

The natural frequencies and mode shapes of a cylinder have been determined in Ref. 28 by using the modal analysis procedure. It is an eigenvalue problem and easy in execution. The effects of imperfection and prestress are considered here, because it has been shown that the fundamental frequency of a cylinder (free of prestress) can be reduced by as much as 65% if certain imperfection shapes are employed.

C. Procedures to Determine Dynamic Critical Loads

The critical conditions are characterized by a large change in dynamic responses for load model 1 and through a plot of load F_{cr} vs duration time T for load model 2. First, consider a cylindrical shell subjected to suddenly applied axial compression or bending moment with finite duration T (load model 1). To get the dynamic critical load, the following three steps are applied.

1) Calculate the frequencies of the cylinder under each load parameter and determine the integration time step according to Eq. (4).

2) Solve the equations of motion for several load parameter values and obtain the dynamic responses.

3) Determine the dynamic critical load as the load at which there is a large change in transient response (see Ref. 16).

Figure 3 presents the dynamic responses of a point on the compressive side of the metallic cylinder subjected to suddenly applied bending moment of finite duration with four load magnitudes. The curve of load $N_b = 6950$ lb (Fig. 3a) is a regular response, and the cylinder vibrates about its equilibrium position. From $N_b = 6981$ to 6985 lb (Figs. 3b and 3c), there is a great change between two responses although the difference in load is only 4 lb or 0.06% of the total load. This is the critical condition according to the Budiansky–Roth[13] criterion and the load average $N_b = 6983$ lb is regarded as the critical dynamic load of the cylinder. Finally, Fig. 3d gives the response curve corresponding to $N_b = 7009$ lb, which is the maximum load that yields the converged dynamic response.

It is found that the dynamic critical loads of a cylinder decrease quickly with increasing load duration and converge to a certain value in the case of load model 1 (Fig. 4). This value is defined as the critical load for the load case of infinite duration (load model 2).

III. Verifications and Results

Numerical results are presented for two distinctly different construction groups. The first one consists of an isotropic cylindrical shell and the second of a laminated shell. The material properties, geometrical properties, and all pertinent information are given for each group.

For the metallic shell (aluminum alloy): $E = 10.5 \times 10^6$ psi, $\mu = 0.3$, $\rho = 2.45 \times 10^{-4}$ lb-s^2/in.^{4}, $0.004 \leq h \leq 0.050$ in., $R = 4$ in., and $L = 4$ in. The metallic shell is simply supported. All of the initial displacements and velocities are set to be zero for the initial conditions. The geometrical imperfection shape is

$$w^0_{(x,\theta)} = ah[-\cos(2\pi x/L) + 0.1\sin(\pi x/L)\cos l\theta] \qquad (5)$$

Note that a is the imperfection amplitude parameter and l the buckling wave number in the circumferential direction. The imperfection shape is taken to be the same as that in Ref. 16, for the purpose of comparing results. It is known from Refs. 25 and 28 that the inward (positive a) and outward (negative a) imperfections have the same influence on the static critical compression loads. For the static bending case, the small outward imperfection ($a = -0.1$) generates a stabilizing effect but is too small to be considered. Therefore, only the inward imperfection is investigated.

The second shell is laminated (boron/epoxy AVCO 5505) with $E_{11} = 30 \times 10^6$, $E_{22} = 2.7 \times 10^6$, and $E_{33} = 2.7 \times 10^6$ psi; $G_{12} = 0.65 \times 10^6$, $G_{13} = 0.65 \times 10^6$, and $G_{23} = 0.37 \times 10^6$ psi; $\mu_{12} = 0.21$, $\mu_{13} = 0.21$, and $\mu_{23} = 0.45$; and $\rho = 1.9134 \times 10^{-4}$ lb-s^2/in.^{4}. The geometrical properties are $R = 7.5$, $L = 7.5$, $h_{\text{ply}} = 0.0053$, and $h = 4h_{\text{ply}} = 0.0212$ in. It is simply supported. All of the initial displacements and velocities are set to be zero for the initial conditions. The stacking sequence is $[45/-45]_s$. The imperfection shape is

$$w^0_{(x,\theta)} = ah\sin\left\{7\pi\left[(x/L) - \tfrac{1}{2}\right]\right\}\cos 4\theta \qquad (6)$$

Table 1 Dynamic critical loads (lb/in.) and pertinent information of verification examples

					Load duration, 10^{-3} s							
R/h	a	l	f, Hz	ΔT, s	1.0	1.25	1.50	1.75	2.00	2.25	Ref. 16	% Difference
1000	0.5	8	580.01	5×10^{-5}	21.4	20.4	19.9	19.7	19.7	19.7	20.4	3.7
500	1.0	8	691.14	5×10^{-5}	48.4	45.7	44.3	43.9	43.8	43.8	46.1	4.9

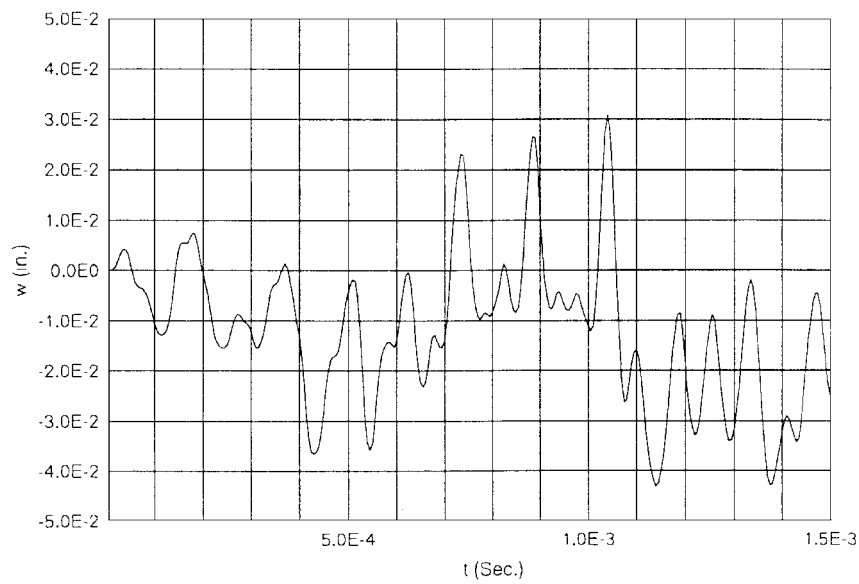

Fig. 3a Dynamic response of the metallic cylinder under bending load N_b = 6950 lb.

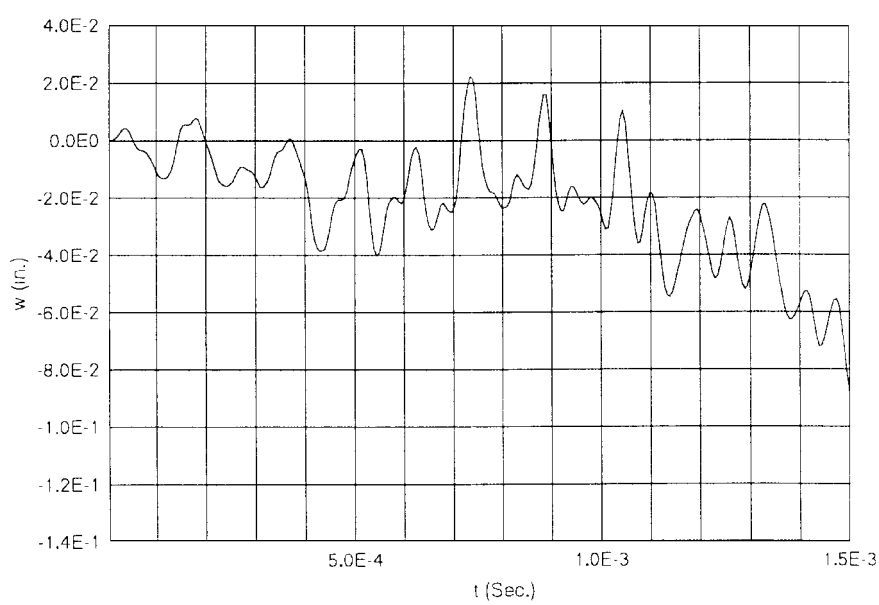

Fig. 3b Dynamic response of the metallic cylinder under bending load N_b = 6981 lb.

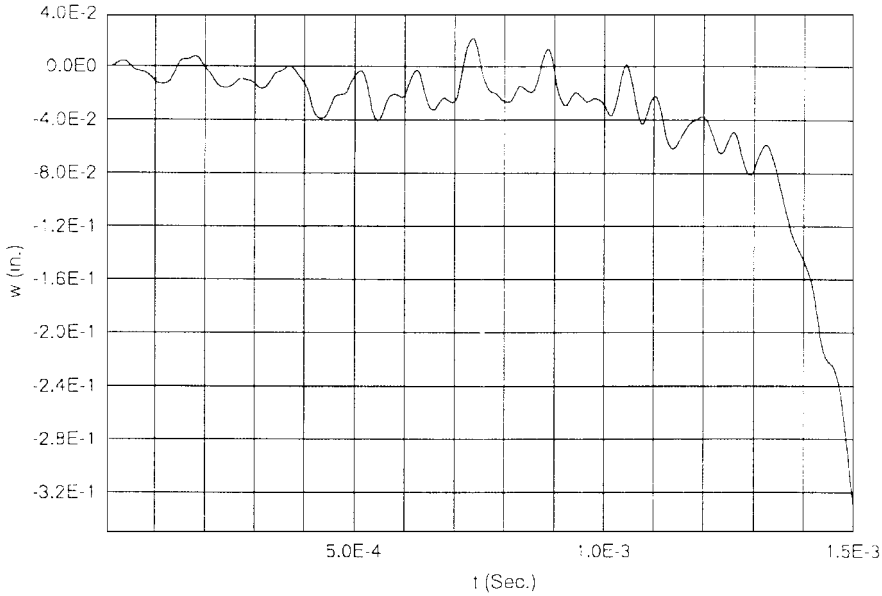

Fig. 3c Dynamic response of the metallic cylinder under bending load N_b = 6985 lb.

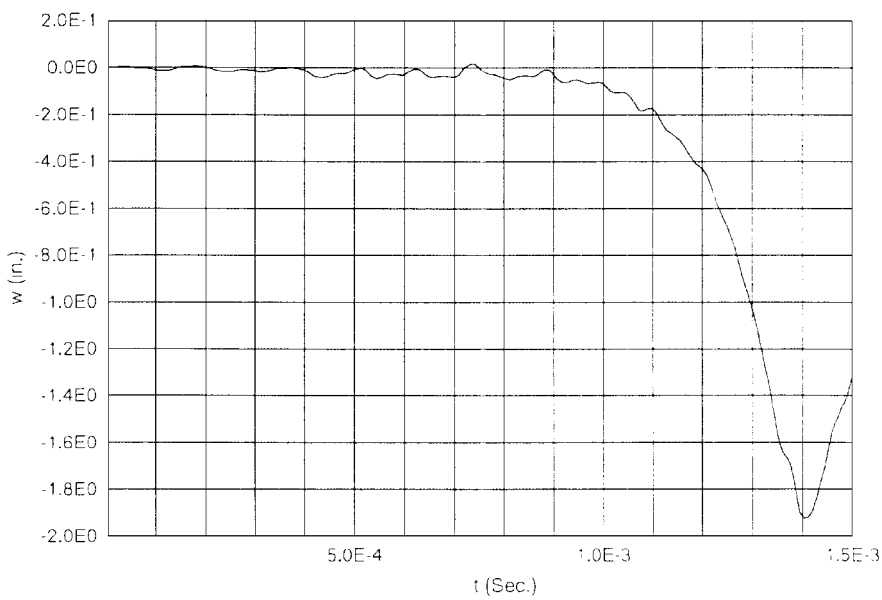

Fig. 3d Dynamic response of the metallic cylinder under bending load N_b = 7009 lb.

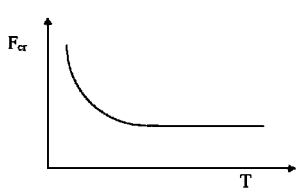

Fig. 4 Dynamic critical loads of finite duration converge to the critical load for the load case of infinite duration.

This imperfection shape is the static linear buckling mode. It is known from static analysis[25] that the cylindrical shell is sensitive to geometric imperfections. An imperfection shape similar to the linear buckling mode yields the lowest critical load. This shape is also used in the dynamic buckling analysis. Note that the cylinder is thin, with a radius-to-thicknessratio $R/h = 354$.

A. Verification Examples

The examples of metallic cylinders under axial compression with different radius-to-thicknessratios and imperfection amplitudes are generated to verify the solution methodology. All dynamical critical loads and pertinent parameters are listed in Table 1. The reference results are taken from Chap. 9 of Ref. 16. They correspond to the load case of infinite duration. The Galerkin procedure and the finite difference method were employed to solve the governing equations. By applying the Hoff–Simitses criterion,[21,22] the dynamic critical loads were determined from the total potential energy of the cylindrical shells. In the present analysis, the integration time step ΔT is assigned as 0.5×10^{-5} s to satisfy Eq. (4) for, at least, the first 10 vibration modes in both examples. It can be seen that the dynamic critical loads converge to 19.7 and 43.8 lb/in., respectively, which are regarded as the critical loads for the load case of infinite duration. The differences between the present and reference results are within 5%.

B. Effect of Load Duration on Dynamic Critical Loads

Tables 2 and 3 list the dynamic critical loads for the metallic cylinder [with $n = 13$, Eq. (5)] subjected to compression and bending moment, respectively. They are also plotted in Figs. 5 and 6 vs the load duration value. The metallic cylinder is relatively thick, with $R/h = 50$. The integration time step ΔT is taken as 5×10^{-6} s. In both load cases, the dynamic critical loads decrease quickly with increasing load duration and converge to critical loads corresponding to the load case of infinite duration.

Table 2 Dynamic critical loads (lb/in.) of the metallic cylinder under compression vs load duration values

T, ms	$a = 0.1$	$a = 0.5$
0.05	25,250.0	18,550.0
0.10	15,370.0	12,150.0
0.50	10,425.0	9,450.0
1.00	9,225.0	7,108.0
1.50	8,173.8	5,600.0
2.00	7,594.0	4,712.0
3.00	6,463.0	4,497.0
4.00	6,463.0	4,497.0
Static	9,008.3	5,675.0
$(N_c)_d/(N_c)_s$[a]	0.72	0.79

[a]Ratio of the dynamic critical compression or bending load for the infinite duration load case to the corresponding static critical load.

Table 3 Dynamic critical loads (lb/in.) of the metallic cylinder under bending vs load duration values

T, ms	$a = 0.1$	$a = 0.5$
0.05	25,425.0	20,930.0
0.10	14,975.0	12,912.0
0.50	7,803.0	6,098.0
1.00	7,012.5	4,197.5
1.50	6,982.5	4,087.0
2.00	6,735.0	3,965.0
2.50	6,682.5	3,940.0
3.00	6,667.5	3,940.0
Static	7,976.7	4,866.7
$(N_b)_d/(N_b)_s$[a]	0.84	0.81

[a]Ratio of the dynamic critical compression or bending load for the infinite duration load case to the corresponding static critical load.

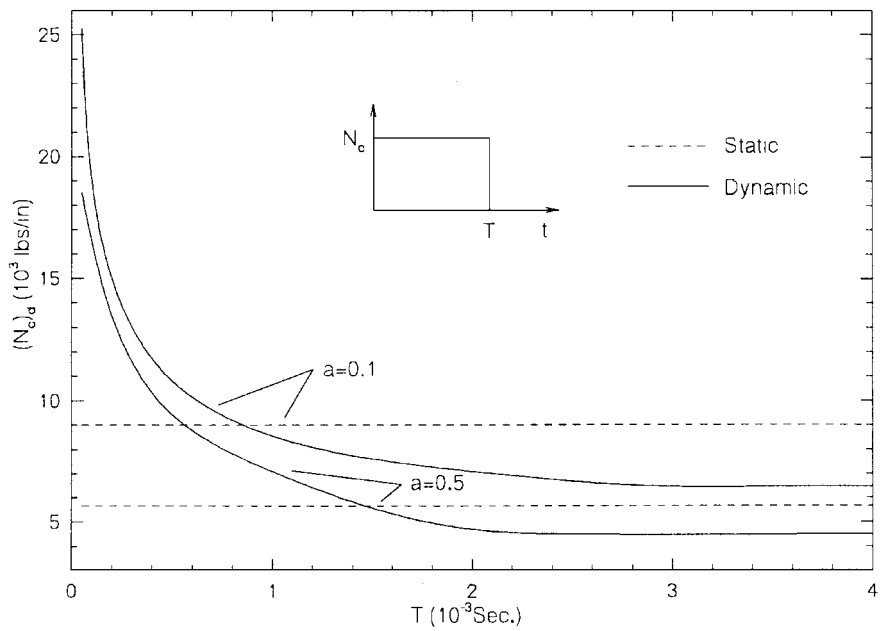

Fig. 5 Dynamic critical compression loads of the metallic cylinder vs load duration.

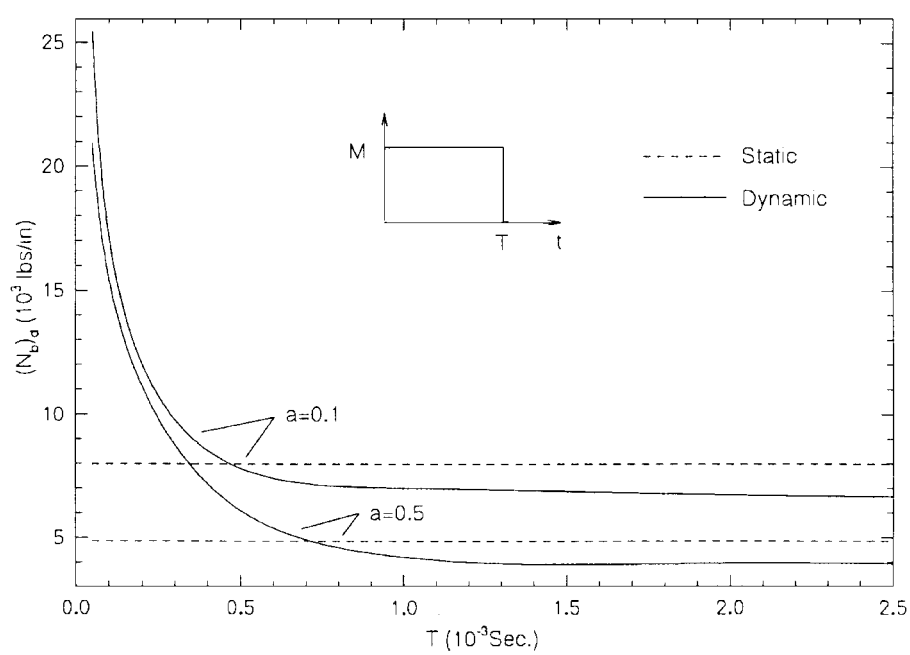

Fig. 6 Dynamic critical bending loads of the metallic cylinder vs load duration.

It can be seen that if the load duration is small the dynamic critical loads are several times higher than the corresponding static critical loads. On the other hand, the critical loads for the infinite duration load case are smaller than the corresponding static critical loads. An attempt is made herein to explain this by taking into consideration the kinematic response as well as the level of the kinetic and potential energies. When a cylindrical shell is suddenly subjected to an axial compression or a bending moment, it begins to vibrate with transverse waves in both the longitudinal and circumferential directions. The wave number and the wavelength depend on the cylinder configuration and the applied load. The larger the applied load, the larger the wave number and the shorter the wavelength. The wave number decreases rapidly with duration time to that of the static buckling mode. Therefore, if the load duration is small, the cylinder has high wave number and short wavelength and, hence, it can withstand larger loads. When the load duration time becomes large, the cylinder vibrates with the static buckling mode. The kinetic energy transfers into potential energy, partly or completely, at some point in time so that the cylinder deforms more than it does under static load with the same magnitude. This makes the cylinder resist a smaller load than the static critical load.

Similar observations hold for the laminated geometry. The results are listed in Tables 4 and 5 and are plotted in Figs. 7 and 8. In the calculation, the integration time step ΔT is taken as 5×10^{-5} s. The convergence rates of dynamic critical loads are related to the fundamental frequencies of cylindrical shells. Table 6 lists the imperfection amplitudes and the fundamental frequencies of the metallic and laminated cylinders. It can be concluded that the larger the frequency, the faster the critical loads converge to the value of the dynamic critical load for the infinite duration case. This is supported by the following.

1) The critical compression and bending loads of metallic cylinders converge after $T = 0.7 \times 10^{-3}$–3.5×10^{-3} s and those for the laminated cylinders after $T \cong 7 \times 10^{-3}$ s because the frequencies of the laminated cylinder are one order of magnitude smaller than those of the metallic cylinder.

2) The frequency of the metallic cylinder with $a = 0.1$ is 2635.6 Hz and with $a = 0.5$ is 2014.0 Hz (Table 6). Consequently, the critical loads for $a = 0.1$ converge faster than those for $a = 0.5$ in Figs. 5 and 6. For the laminated cylinders, the frequencies are almost independent of imperfection amplitude values and, hence, the critical loads reduce at the same rate. In addition, the critical bending

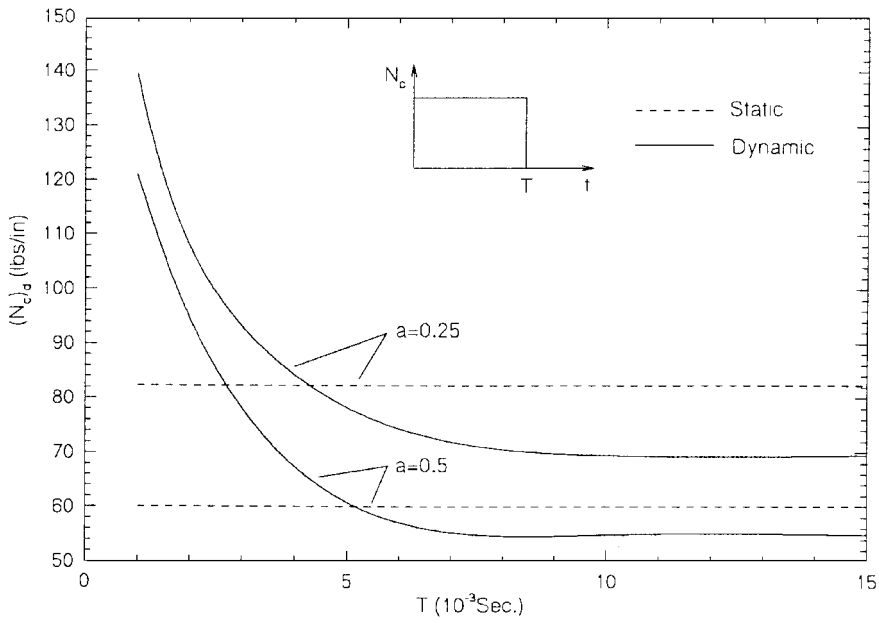

Fig. 7 Dynamic critical compression loads of the laminated cylinder vs load duration.

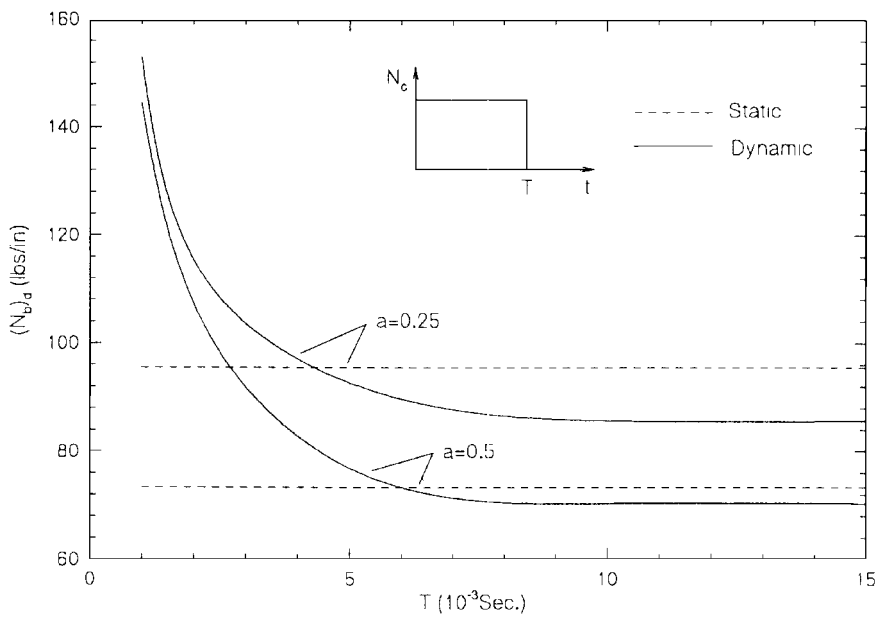

Fig. 8 Dynamic critical bending loads of the laminated cylinder vs load duration.

loads converge faster than the critical compression loads for the metallic cylinder.

For the load case of infinite duration, the dynamic critical loads are always smaller than the corresponding static critical loads. The ratios of dynamic critical loads to static critical load range from 0.72 to 0.96 in the studied cases. The ratios of critical bending stresses are larger than those of compression stresses for both the metallic cylinder and the laminated cylinder. Hence, the differences of dynamic and static critical loads for bending case are smaller than those for compression case. Also, these differences are larger for the metallic cylinder than those for the laminated cylinder.

C. Effect of Imperfection Amplitudes on Critical Loads

The static and dynamic critical loads of the metallic cylinder are listed in Tables 7 and 8. They are also described in Figs. 9 and 10 vs imperfection amplitudes and load duration values for compression and bending cases, respectively. Those for the laminated cylinder are presented in Tables 9 and 10 and plotted in Figs. 11 and 12. Both static and dynamic critical loads decrease with increasing imperfection amplitude for all configurations. The rate depends on the load duration, and the longer the load duration is, the larger the rate of decrease. In addition, the static critical loads decrease faster than the dynamic critical loads. For example, in the bending case of the metallic cylinder, the critical loads for $a = 1.0$ are 0.51, 0.41, 0.39, and 0.35 of those for $a = 0.0$ and for load duration values of $T = 0.5$, 1.0, 2.0 ms and the static case, respectively.

Table 4 Dynamic critical loads (lb/in.) of the laminated cylinder under compression vs load duration values

T, ms	$a = 0.25$	$a = 0.5$
1.00	139.5	121.0
2.50	99.50	85.50
5.00	78.25	57.75
10.0	69.51	54.88
15.0	69.51	54.88
Static	82.22	60.05
$(N_c)_d/(N_c)_s$[a]	0.85	0.91

[a]Ratio of the dynamic critical compression or bending load for the infinite duration load case to the corresponding static critical load.

Table 5 Dynamic critical loads (lb/in.) of the laminated cylinder under bending vs load duration values

T, ms	$a = 0.25$	$a = 0.5$
1.00	153.0	144.5
2.50	108.5	98.50
5.00	92.70	77.00
10.0	85.65	70.35
15.0	85.65	70.35
Static	95.56	73.33
$(N_b)_d/(N_b)_s$[a]	0.90	0.96

[a]Ratio of the dynamic critical compression or bending load for the infinite duration load case to the corresponding static critical load.

Table 6 Fundamental frequencies of cylindrical shell

Metallic cylinder		Laminated cylinder	
a	f, Hz	a	f, Hz
0.00	2793.3	0.00	490.3
0.10	2635.6	0.05	490.1
0.25	2381.0	0.10	489.7
0.50	2014.0	0.25	486.6
1.00	1630.9	0.50	477.7

Table 7 Dynamic critical loads (lb/in.) of the metallic cylinder under compression vs imperfection amplitudes and load duration values

a	0.5 ms	1.0 ms	2.0 ms	Static
0.0	10,809.0	10,360.0	8,319.60	9,871.40
0.1	10,425.5	9,225.00	7,595.75	9,008.3
0.5	9,450.00	7,108.00	4,712.00	5,675.00
1.0	8,498.90	5,774.80	3,850.40	4,475.00
RA1[a]	0.80	0.54	0.47	0.45

[a]Ratio of the critical load for $a = 1.0$ to the critical load for $a = 0.0$.

Table 8 Dynamic critical loads (lb/in.) of the metallic cylinder under bending load vs imperfection amplitudes and load duration values

a	0.5 ms	1.0 ms	2.0 ms	Static
0.0	9000.0	7275.0	7112.5	9236.7
0.1	7803.0	7012.5	6735.0	7976.7
0.5	6098.0	4197.5	3965.0	4866.7
1.0	4600.0	3000.0	2800.0	3206.7
RA1[a]	0.51	0.41	0.39	0.35

[a]Ratio of the critical load for $a = 1.0$ to the critical load for $a = 0.0$.

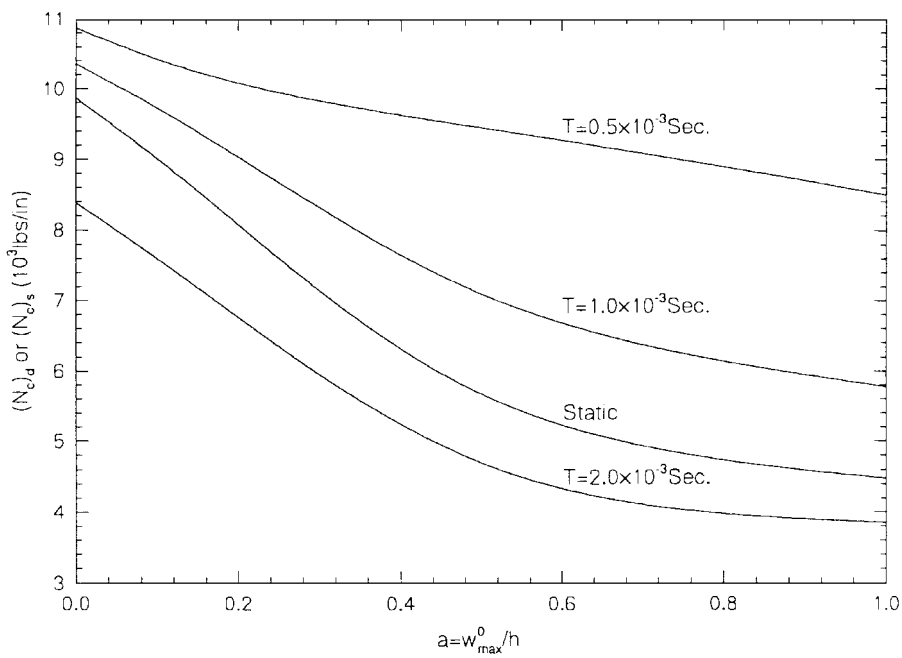

Fig. 9 Critical compression loads of the metallic cylinder vs imperfection amplitudes.

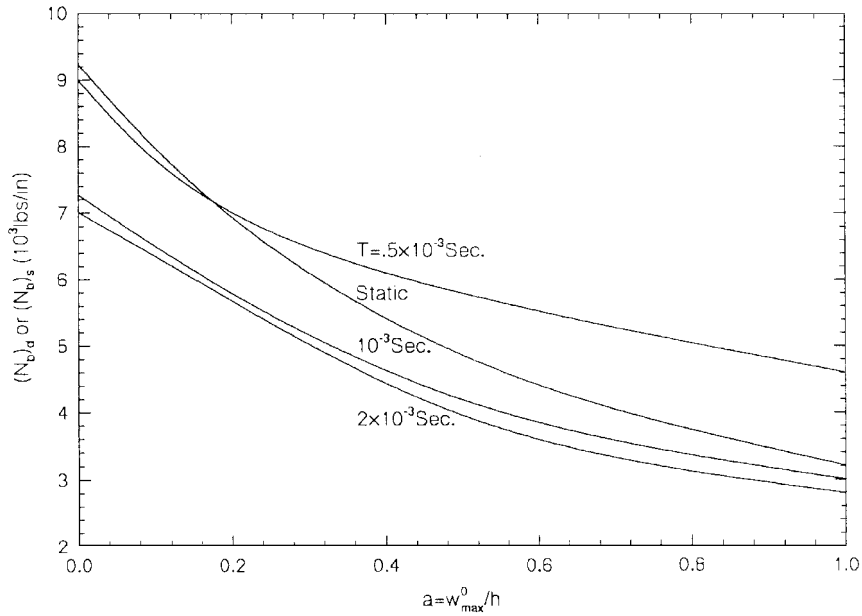

Fig. 10 Critical bending loads of the metallic cylinder vs imperfection amplitudes.

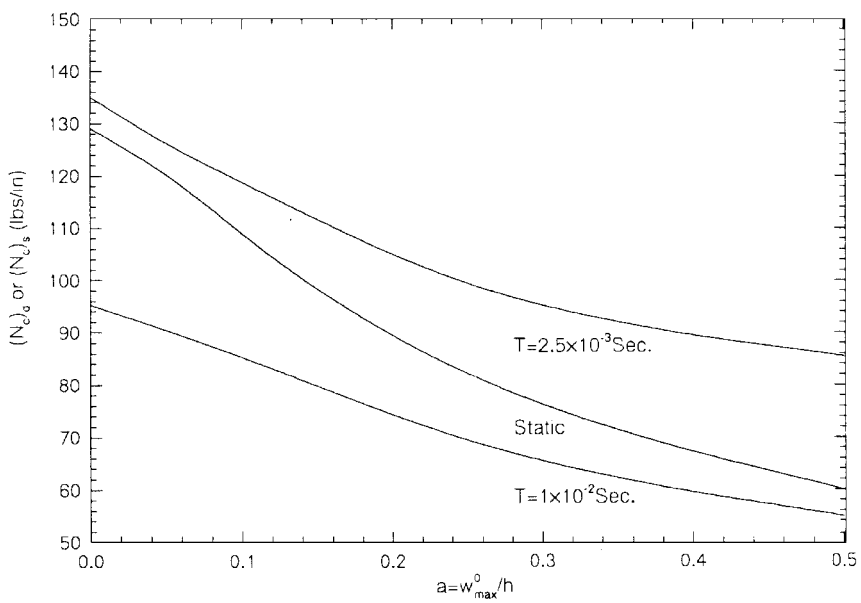

Fig. 11 Critical compression loads of the laminated cylinder vs imperfection amplitudes.

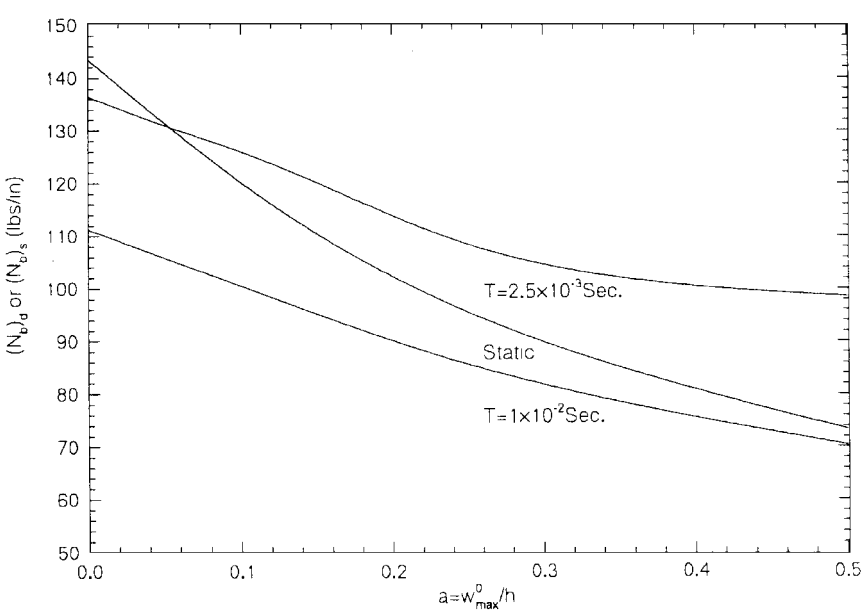

Fig. 12 Critical bending loads of the metallic cylinder vs imperfection amplitudes.

Table 9 Dynamic critical loads (lb/in.) of the laminated cylinder under compression vs imperfection amplitudes

a	2.5 ms	10 ms	Static
0.00	135.0	101.6	129.1
0.05	126,3	95.24	120.2
0.10	118.8	89.25	108.9
0.25	99.50	69.51	82.22
0.50	85.50	54.88	60.05
RA2[a]	0.63	0.54	0.46

[a]Ratio of the critical load for $a = 0.5$ to the critical load for $a = 0.0$.

Table 10 Dynamic critical loads (lb/in.) of the laminated cylinders under bending moment vs imperfection amplitudes

a	2.5 ms	10 ms	Static
0.00	136.5	111.3	143.5
0.05	131.0	109.75	131.1
0.10	126.0	105.0	120.2
0.25	108.5	85.65	95.56
0.50	98.50	70.35	73.33
RA2[a]	0.72	0.63	0.51

[a]Ratio of the critical load for $a = 0.5$ to the critical load for $a = 0.0$.

IV. Conclusion

1) The equations of motion approach (Budiansky–Roth[13]) is successfully applied to calculate the dynamic critical loads of imperfect circular cylindrical shells subjected to suddenly applied axial compression and bending moment with finite and infinite duration. This method is easily adapted to computational tools such as finite element codes and has met with success when applied to systems that exhibit violent buckling under static loads.

2) The dynamic critical loads are strongly dependent on the load duration. They decrease rapidly with increasing load duration in all cases and converge to those corresponding to the load case of infinite duration. The convergence rate depends on the fundamental frequencies: the larger the fundamental frequency, the faster the critical loads converge.

3) The imperfect shape has significant effect on static critical loads, and the worst shape is the one corresponding to the linear buckling mode.[25] For both metallic and laminated cylindrical shells, the static and dynamic critical loads reduce with increasing imperfection amplitude in both cases of compression and of bending.

Acknowledgments

This work is supported by the Office of Naval Research under Grant 0014-95-0597. Their financial support is gratefully acknowledged. In addition, the support provided by the Ohio Supercomputer Center in terms of time on the Cray YMP8E under Grant PES443-5 is also appreciated.

References

[1]Bolotin, V. V., *The Dynamic Stability of Elastic Systems*, Holden-Day, San Francisco, 1964 (translated by V. I. Weingarten, L. B. Greszczuk, K. N. Trirogoff, and K. D. Gallegos).

[2]Kovtunov, V. B., "Dynamic Stability and Nonlinear Parametric Vibration of Cylindrical Shells," *Computers and Structures*, Vol. 46, No. 1, 1985, pp. 149–156.

[3]Argento, A., and Scott, R. A., "Dynamic Instability of Layered Anisotropic Circular Cylindrical Shells, Part I: Theoretical Development," *Journal of Sound and Vibration*, Vol. 162, No. 2, 1993, pp. 311–322.

[4]Lindberg, H. E., and Florence, A. L., *Dynamic Pulse Buckling*, Martinus Nijhoff, Boston, MA, 1987.

[5]Pegg, N. G., "A Numerical Study of Dynamic Pulse Buckling of Ring-Stiffener Cylinders," *Computers and Structures*, Vol. 44, No. 6, 1992, pp. 1205–1214.

[6]Kirkpatrik, S. W., and Holmes, B. S., "Effect of Initial Imperfections on Dynamic Buckling of Shells," *Journal of Engineering Mechanics*, Vol. 115, No. 5, 1989, pp. 1075–1093.

[7]Paidoussis, M. P., "Flow-Induced Instabilities of Cylindrical Structures," *Applied Mechanics Reviews*, Vol. 40, No. 2, 1987, pp. 163–175.

[8]Svalbonas, V., and Kalnins, A., "Dynamic Buckling of Shells: Evaluation of Various Methods," *Nuclear Engineering and Design*, Vol. 44, No. 3, 1977, pp. 331–356.

[9]Hsu, C. S., "On Parametric Excitation and Snap-Through Stability Problems of Shells," *Thin-Shell Structures*, edited by Y. C. Fung and E. E. Sechler, Prentice–Hall, Englewood Cliffs, NJ, 1974, pp. 103–131.

[10]Simitses, G. J., "Instability of Dynamically-Loaded Structures," *Applied Mechanics Reviews*, Vol. 40, No. 10, 1987, pp. 1403–1408.

[11]Volmir, A. S., "On the Stability of Dynamically Loaded Cylindrical Shells," *Doklady Academi Nauk SSSR*, Vol. 123, No. 5, 1958, pp. 806–808 (in Russian); translated in *Soviet Physics-Doklady*, Vol. 3, 1958, pp. 1287–1289.

[12]Roth, R. S., and Klosner, J. M., "Nonlinear Responses of Cylindrical Shells Subjected to Dynamic Axial Loads," *AIAA Journal*, Vol. 12, No. 10, 1964, pp. 1788–1794.

[13]Budiansky, B., and Roth, R. S., "Axisymmetric Dynamic Buckling of Clamped Shallow Spherical Shells," *Collected Papers on Instability of Shell Structures*, NASA TN D-1510, 1962, pp. 597–606.

[14]Tamura, Y. S., and Babcock, C. D., "Dynamic Stability of Cylindrical Shells Under Step Loading," *Journal of Applied Mechanics*, Vol. 42, No. 1, 1975, pp. 190–194.

[15]Simitses, G. J., "Effect of Static Preloading on the Dynamic Stability of Structures," *AIAA Journal*, Vol. 21, No. 8, 1983, pp. 1174–1180.

[16]Simitses, G. J., *Dynamic Stability of Suddenly Loaded Structures*, Springer–Verlag, New York, 1985.

[17]Kounadis, A. N., "Nonlinear Dynamic Buckling of Discrete Dissipative or Nondissipative Systems Under Step Loading," *AIAA Journal*, Vol. 29, No. 2, 1991, pp. 281–289.

[18]Kounadis, A. N., "On the Nonlinear Dynamic Buckling Mechanism of Autonomous Dissipative/Nondissipative Discrete Structural System," *Archive of Applied Mechanism*, Vol. 66, No. 2, 1996, pp. 395–408.

[19]Hsu, C. S., "On Dynamic Stability of Elastic Bodies with Prescribed Initial Conditions," *International Journal of Engineering Science*, Vol. 4, No. 1, 1966, pp. 1–21

[20]Hsu, C. S., "The Effects of Various Parameters on the Dynamic Stability of a Shallow Arch," *Journal of Applied Mechanics*, Vol. 34, No. 2, 1967, pp. 349–356.

[21]Hoff, N. J., and Bruce, V. C., "Dynamic Analysis of the Buckling of Laterally Loaded Flat Arches," *Journal of Mathematical Physics*, Vol. 32, 1954, pp. 276–288.

[22]Simitses, G. J., "Dynamic Snap-Through Buckling of Low Arches and Shallow Spherical Capes," Ph.D. Dissertation, Dept. of Aeronautics and Astronautics, Stanford Univ., Stanford, CA, June 1965.

[23]Palazotto, A. N., and Dennis, S. T., *Nonlinear Analysis of Shell Structures*, AIAA, Washington, DC, 1993.

[24]Ahmad, S., Irons, B. M., and Zienkiewicz, O. C., "Analysis of Thick and Thin Shell Structures by Curved Finite Element," *International Journal for Numerical Methods in Engineering*, Vol. 2, No. 4, 1970, pp. 419–451.

[25]Huyan, X., Simitses, G. J., and Tabiei, A., "Nonlinear Analysis of Imperfect Metallic and Laminated Cylinders Under Bending Loads," *AIAA Journal*, Vol. 34, No. 11, 1996, pp. 2406–2413.

[26]Cook, R. D., Malkus, D. S., and Plesha, M. E., *Concepts and Applications of Finite Element Analysis*, 3rd ed., Wiley, New York, 1989.

[27]Swanson, "ANSYS User's Manual for Revision 5.0," Swanson Analysis System, Houston, PA, Dec. 1992.

[28]Huyan, X., "Dynamic Stability of Cylindrical Shells of Various Constructions," Ph.D. Dissertation, Dept. of Aerospace Engineering and Engineering Mechanics, Univ. of Cincinnati, Cincinnati, OH, June 1996.

G. A. Kardomateas
Associate Editor